symmetry

MDPI

Article

Searching for Orbits for a Mission to the Asteroid 2001SN$_{263}$ Considering Errors in the Physical Parameters

Allan Kardec de Almeida Junior [1,*], Bruna Yukiko Pinheiro Masago Mescolotti [1], Ana Paula Marins Chiaradia [2], Vivian M. Gomes [2] and Antonio Fernando Bertachini de Almeida Prado [1,3]

[1] Instituto Nacional de Pesquisas Espaciais-INPE, Divisão de Pós-Graduação, Av. dos Astronautas, 1758, São José dos Campos 12227-010, Brazil
[2] Department of Mathematics, Universidade Estadual Paulista-UNESP, Av. Ariberto Pereira da Cunha, 333, Guaratinguetá 12516-410, Brazil
[3] Academy of Engineering, RUDN University, Miklukho-Maklaya Street 6, 117198 Moscow, Russia
* Correspondence: fenixcinza@yahoo.com.br

Abstract: The main goal of this paper is to search for orbits that can be used in the Brazilian proposed Aster mission. This mission is under study and its objective is to use a spacecraft to observe the system 2001SN$_{263}$, which is a triple asteroid system. With respect to the two-body problem (spacecraft and the main asteroid), the symmetries of the orbits are broken by the oblateness of the main body of the system, the solar radiation pressure, and the gravitational attraction of the two moons of the main body. Additionally, the masses of these two moons have errors associated with their predicted values, which reinforce the asymmetry and require extra effort to maintain the observational objectives of the mission. The idea is to find orbits that remain for some time observing the three bodies of that system, even if the physical parameters of the bodies are not the ones expected from observations made from the Earth. This is accomplished by studying the effects of errors in all the physical properties of the three asteroids in the trajectories described by a spacecraft that is orbiting this system. Several important and useful trajectories are found, which are the ones that can observe the desired bodies, even if the physical parameters are not the expected ones. To express our results, we built time histories of the relative distances between each of the asteroids and the spacecraft. They are used to select the trajectories according to the amount of time that we need to observe each body of the system. In this way, the first objective of this research is to search for trajectories to keep the spacecraft close to the three bodies of the system as long as possible, without requiring orbital maneuvers. The errors for the masses of the two smaller and lesser known bodies are taken into consideration, while the mass of the most massive one is assumed to be known, because it was determined with higher precision by observations.

Keywords: astrodynamics; asteroid 2001SN263; errors in the physical parameters; observational mission; Aster mission

Citation: de Almeida Junior, A.K.; Mescolotti, B.Y.P.M.; Chiaradia, A.P.M.; Gomes, V.M.; de Almeida Prado, A.F.B. Searching for Orbits for a Mission to the Asteroid 2001SN$_{263}$ Considering Errors in the Physical Parameters. *Symmetry* **2022**, *14*, 1789. https://doi.org/10.3390/sym14091789

Academic Editor: Jan Awrejcewicz

Received: 25 July 2022
Accepted: 24 August 2022
Published: 28 August 2022

1. Introduction

The scientific literature indicates that many answers about the origin and evolution of our solar system may be found in smaller bodies. In that sense, a key factor for a better understanding of our solar system is space missions to asteroids. They are small bodies, with many of them located between the orbits of Mars and Jupiter. Some asteroids pass by the neighborhood of the Earth, and they are the called near-Earth asteroids (NEAs). We already have many spacecrafts (and missions) that have explored these bodies, such as the Galileo [1–3]; the NEAR Shoemaker spacecraft [4,5]; the hovering at the asteroid (25143) Itokawa [6]; a vision to explore the deep space [7]; the Hayabusa mission [8]; missions to visit the 2001 SN263 asteroid, including the Aster [9] and the Amor [10]; the 162173 (1999 JU3) asteroid [11]; the European MarcoPolo-R with sample return mission [12]; the Hayabusa 2 [13]; the OSIRIS-Rex mission to Bennu [14–16]; and analyses on general small

bodies missions [17]. Apart from this research which is related to specific missions, some other publications have studied orbits around small bodies, and they can be used in future missions. Some of them are: [18–31].

Having the goal of studying asteroids in deeper detail, the Brazilian Aster mission was proposed and studied from several different aspects. Its objective is to place a spacecraft in orbit of the triple asteroid system $2001SN_{263}$. Several schemes are considered: serial, in which the spacecraft visits one body after the other; parallel, in which all the bodies are observed from a single orbit; and hybrid, which combines both strategies, alternating orbits using propulsion. In that sense, the present paper contributes by showing orbits that can be used to observe each of the single orbits, two of them, or even all the bodies of the system. Several previous studies approached this mission from different perspectives. For more details, one can refer to: [9,10,32–39].

The central gravitational attraction of the main body is the most important force acting on a spacecraft in orbit. The two-body problem describes the motion of a spacecraft under such force, which is symmetric, and its orbits are usually periodic. In comparison with the orbit modeled by the two-body problem, the solar radiation pressure alone may not be enough to break the symmetry of the orbit [40]. On the other side, when the spacecraft has close encounters with the smaller bodies of the 2001 SN263 system, which is the objective of an observational mission, their gravitational forces generate asymmetries, which must be taken into consideration when selecting the final trajectories. The weak gravitational fields of the moons are responsible for non-Keplerian orbits around them. The simplified Keplerian model does not give a minimum acceptable accuracy. Furthermore, for orbits near the main body, its non-perfect spherical shape perturbs the symmetry of the orbit. In order to try to solve this problem, there are several researchers looking for stable trajectories around non-perfect spherical bodies [41–43].

Looking at a different aspect, the main goal of the present paper is to observe the effects of the errors in the masses of the two smaller bodies in the observational times, which are the times that the spacecraft remains near the bodies of the system. The information about the masses of the bodies is not very accurately known, and better values will be available only when the spacecraft gets closer to the bodies. So a study is made in the present paper to verify what happens to the observation times of a trajectory that is designed using the nominal values for the masses, but is governed by the real values. By performing this type of study, it is possible to find orbits that are less sensitive to those parameters, keeping some observational times even if the masses are not what were expected before the arrival of the spacecraft. Those orbits are very important to place the spacecraft in the beginning of the mission, before a better determination of the masses is made. This research is an extension of a previous paper [35] that studied a similar problem in a double asteroid system.

2. The Triple Asteroid $2001SN_{263}$

This system of multiple asteroids is considered one of the most interesting set of bodies of the solar system to be visited. It is a triple system that is part of the group that is called NEAs (near-Earth asteroids). It was discovered by the Arecibo Observatory in 2008. Several observations were required after it was discovered to make sure it was a triple system and not a single body [44]. It is formed by a larger main body called Alpha with a diameter of 2.6 km and two smaller companions (called Beta and Gamma), with diameters of 0.78 km and 0.58 km, respectively, which are orbiting Alpha. Table 1 gives the physical data and the Keplerian elements of the all the three bodies [32,33]. In Table 1, a represents the semi-major axis, e the eccentricity, and i the inclination of the orbits involved.

Table 1. Physical data and Keplerian Elements of the asteroids of the system 2001SN263 [32,33].

Body	Central Body	a	e	i	Period	Radius (km)	Mass ($\times 10^{10}$ kg) [33]
Alpha	Sun	1.99 AU	0.48	6.7°	2.80 years	1.30	$m_\alpha = 917.466 \pm 2.235$
Beta	Alpha	16.633 km	0.015	0.00°	6.23 days	0.39	$m_\beta = 24.039 \pm 7.531$
Gamma	Alpha	3.804 km	0.016	13.87°	0.69 days	0.29	$m_\gamma = 9.773 \pm 3.273$

3. Description of the Problem

The priority of the present research is to study the effects of different values for the masses of the two smaller bodies of the system in the trajectories of a spacecraft orbiting those asteroids. The errors for Beta and Gamma are 31% and 33% of their masses, respectively, while the error for the most massive body (Alpha) is only 0.24% of its mass, as can be seen in Table 1. Thus, in this research, the mass of Alpha is assumed to be known, as there is much more information available about this body in comparison to what is known about the two smaller ones. In particular, the trajectories found here are compared with the ones available in [35] as a function of those errors. Of course, we pay more attention to trajectories that can observe at least two or even three of the bodies of the system. We define a distance of five kilometers from the center of each body as a good value for observations, based on the experiments planned. It means that this research measures the length of time the spacecraft stays inside this limit of five kilometers from each asteroid. The effects of the errors in the masses of the bodies over those observation times are investigated.

The model for the dynamics used in the numerical simulations considers all the information available about the system $2001SN_{263}$. It includes their sizes, masses, and shapes. Solar radiation pressure is also included in the equations of motion, because this is an important force near small bodies due to their weak gravity fields. It is also assumed that the smaller bodies are in precessing elliptical orbits around Alpha, due to the non-spherical shape of the central body. The oblateness of the central body is also included in the calculation of the trajectories of the spacecraft.

A local frame of reference centered in the barycenter of the triple system is defined. In this research, this local frame is considered as an inertial one. In the case in which the Sun is taken into consideration, this local frame of reference becomes a non-inertial one. In this case, the magnitude of the specific force due to the influence of the Sun over the spacecraft is given by $p_s = \mu_s \left| \boldsymbol{r}_s / r_s^3 + \boldsymbol{R}_s / R_s^3 \right|$, where μ_s is the gravitational parameter of the Sun, $\boldsymbol{R}_s$ locates the Sun from the center of the non-inertial frame of reference, and $\boldsymbol{r}_s = \boldsymbol{r}' - \boldsymbol{R}_s$, where $\boldsymbol{r}' = (x', y', z')$ is the position of the spacecraft in the non-inertial frame. Details on how this term is derived can be seen in [45]. Note that p_s compares the specific force due to the Sun over the spacecraft using the frame of reference centered in the triple system when it is considered an inertial one (the case adopted in this work) with the same frame of reference when it is considered a non-inertial one (rotating around the Sun). The magnitude of the acceleration due to the Sun given by p_s and the magnitudes of the gravitational accelerations due Alpha, Beta, and Gamma are shown in Figure 1 as functions of x' (for $y' = z' = 0$) in the case in which Alpha, Beta, and Gamma are aligned in the positive side of the x' axis. This figure shows their levels of influence over the dynamics of the spacecraft. Note that the gravitational influences of Alpha, Beta, and Gamma are very strong close to each of them, respectively. Thus, they could not be neglected. On the other side, in the region close to the triple system, p_s is at least four orders of magnitude lower than the magnitude of the gravitational attraction of Alpha and at least two orders of magnitude lower than the magnitudes of the gravitational attractions of Beta and Gamma. Hence, the influence of the Sun over the dynamics of a spacecraft close to the triple system is negligible for integration times of the order of days, as the ones used in this research. Therefore, the adoption of the inertial frame of reference fixed in the barycenter of the triple asteroid system is suitable for the purposes of this research. Other perturbations were considered too small to be included in the mathematical model.

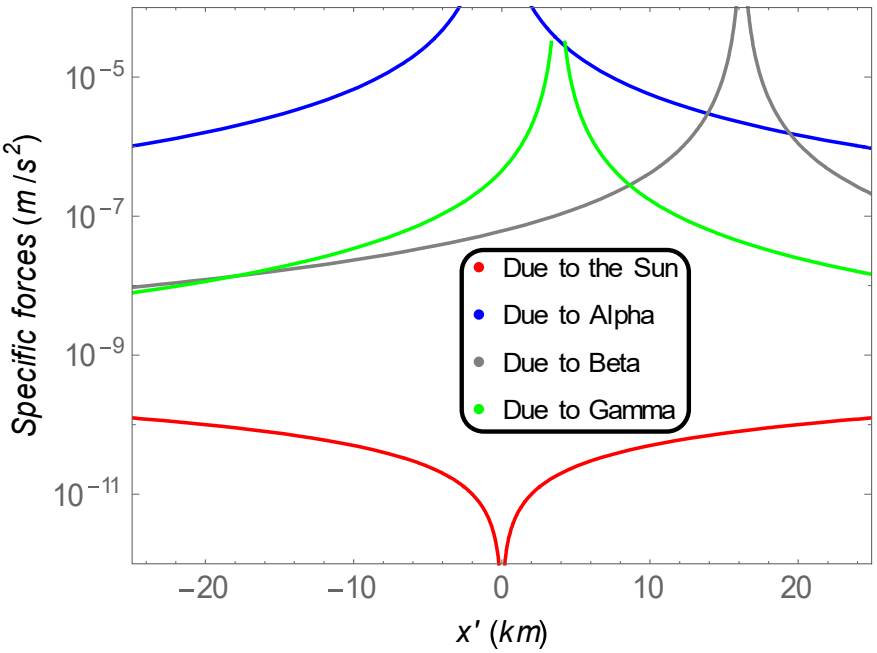

Figure 1. Comparisons among the specific forces.

A change in coordinates is used from the local frame of reference defined above such that another system of reference based in the orbital plane of Beta is used. Combined with a Taylor expansion of the Kepler's equation, this change in coordinates allowed us to obtain analytical approximated solutions to the elliptical motion of the massive bodies, which helped to obtain much faster numerical solutions to the motion of the spacecraft.

It is known that there are orbits around the central body that can be used to observe all three bodies of the system [35]. We used the best orbits shown in [35] for particular studies.

4. Equations of Motion

To study the proposed problem, it is necessary to write equations of motion for the spacecraft that are not too complex, but that are accurate enough to reveal the main characteristics of the orbits. Our main assumption is that the spacecraft moves under the forces given by the gravitational field of the three asteroids, the flattening of the largest body, and the effects of solar radiation pressure. The first step is to use Equations (1)–(3) to obtain the distances between the spacecraft and the three asteroids. We define R_1 as the distance between Alpha and the spacecraft; R_2 as the distance between Beta and the spacecraft; R_3 as the distance between the spacecraft and Gamma; and R as the distance between the spacecraft and the center of the frame of reference. The massive bodies of the triple system, the spacecraft, and the variables are shown in Figure 2.

$$R_1 = \sqrt{(x - x_\alpha)^2 + (y - y_\alpha)^2 + (z - z_\alpha)^2} \tag{1}$$

$$R_2 = \sqrt{(x - x_\beta)^2 + (y - y_\beta)^2 + (z - z_\beta)^2} \tag{2}$$

$$R_3 = \sqrt{(x - x_\gamma)^2 + (y - y_\gamma)^2 + (z - z_\gamma)^2} \tag{3}$$

The correct calculation of those three variables is very important, because they appear in the equations of motion and they constitute the main criterion to select the best orbits. After these definitions have been established, we can use the inertial frame to write the equations of motion of the spacecraft, which are given by Equations (4)–(6) [35].

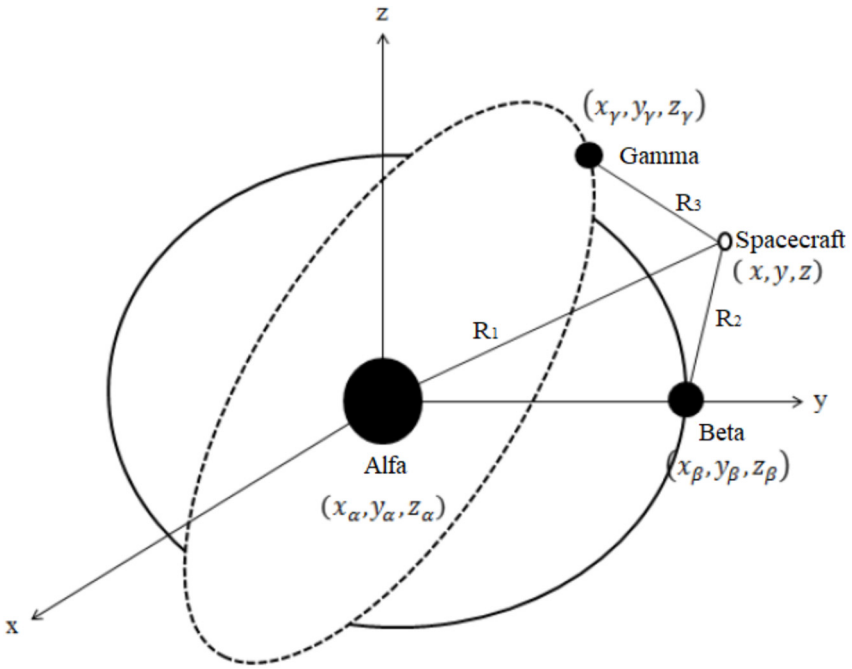

Figure 2. The triple asteroid system and the spacecraft.

$$\ddot{x} = -\mu_\beta \frac{(x - x_\beta)}{{R_1}^3} - \mu_\gamma \frac{(x - x_\gamma)}{{R_2}^3} - \mu_\alpha \frac{(x - x_\alpha)}{{R_3}^3} - \mu_\alpha J_2 {r_\alpha}^2 \left(\frac{3x}{2r^5} - \frac{15z^2 x}{2r^7} \right) + P_{radx} \quad (4)$$

$$\ddot{y} = -\mu_\beta \frac{(y - y_\beta)}{{R_1}^3} - \mu_\gamma \frac{(y - y_\gamma)}{{R_2}^3} - \mu_\alpha \frac{(y - y_\alpha)}{{R_3}^3} - \mu_\alpha J_2 {r_\alpha}^2 \left(\frac{3y}{2r^5} - \frac{15z^2 y}{2r^7} \right) + P_{rady} \quad (5)$$

$$\ddot{z} = -\mu_\beta \frac{(z - z_\beta)}{{R_1}^3} - \mu_\gamma \frac{(z - z_\gamma)}{{R_2}^3} - \mu_\alpha \frac{(z - z_\alpha)}{{R_3}^3} - \mu_\alpha J_2 {r_\alpha}^2 \left(\frac{9z}{2r^5} - \frac{15z^3}{2r^7} \right) + P_{radz} \quad (6)$$

where $J_2 = 0.013$ is obtained in [33] though orbit-fitting; P_{radx}, P_{rady} and P_{radz} represent the x, y and z components of the acceleration given by the solar radiation pressure; r_α is the radius of Alpha; and μ_α, μ_β, and μ_γ are the gravitational parameters (the multiplication of the mass by the universal gravitational constant) of the bodies involved. To model the acceleration giving by the solar radiation pressure force, we use Equation (7) shown as:

$$P = \frac{h(1+\epsilon)}{c} \frac{S}{m} \left(\frac{r_0}{R} \right)^2 \cos\alpha^2 \quad (7)$$

where S represents the cross-section area of the spacecraft that is illuminated by the Sun; h = 1360 W/m^2 is the solar radiation constant for a spacecraft travelling near the Earth; r_0 is the Earth–Sun distance; R is the spacecraft–Sun distance; ϵ is the reflectivity coefficient; c is the speed of light; m is the mass of the spacecraft; and α is the angle of the incident light [46]. The value used for the numerical simulations for the area to mass ratio (S/m) of the spacecraft was 0.01 m^2/kg.

5. Results

To start our studies, the initial conditions for the orbits are calculated based in the mathematical model given by the two-body problem (spacecraft-Alpha). Those calculations are performed to find initial orbits that generate repeated passages of the spacecraft by the body under observation. Good candidates for first orbits are the ones which are resonant with the orbital period of Beta and Gamma [35].

After that, those orbits are integrated numerically using the mathematical model explained above. It also verified the occurrence of collisions of the spacecraft with one of the bodies of the system. As already explained, the distances R_1, R_2, and R_3 are calculated all the time, as well as the durations of the passages of the spacecraft below the limit of 5 km from the center of the bodies.

The estimated errors in the masses of both smaller bodies of the system are now considered [33] and, from these errors, nine scenarios are possible after combining the possibilities of maximum positive (+), minimum negative (−), or zero average (0) errors for the mass of Beta and Gamma, according to their values shown in Table 1. Detailed information of all the possible combinations is shown in Table 2. The first column gives an identification number for the scenario; the second column indicates if the masses of the smaller primaries have positive, negative, or zero error. The value for β is on the left side while the value of γ is on the right side. The third column describes the errors.

Table 2. Scenarios simuladed.

Scenario	Symbol	Nomenclature
1	(+) (+)	m_β + error, m_γ + error
2	(+) (0)	m_β + error, m_γ without error
3	(+) (−)	m_β + error, m_γ − error
4	(0) (+)	m_β without error, m_γ + error
5	(0) (0)	m_β without error, m_γ without error
6	(0) (−)	m_β without error, m_γ − error
7	(−) (+)	m_β − error, m_γ + error
8	(−) (0)	m_β − error, m_γ without error
9	(−) (−)	m_β − error, m_γ − error

Two different possibilities are used for the relative positions of the smaller asteroids: when they are on the same side relative to Alpha, they are named "same side geometry"; and when they are in opposite directions, they are named "opposite geometry" [35]. The geometry is constructed with the asteroid at the periapsis (true anomaly 0°) or apoapsis (true anomaly 180°) of its orbit around the Sun. This is an important factor, because the large eccentricity of the orbit of the asteroid (0.48) changes the effects of the solar radiation pressure as a function of its true anomaly. The nomenclature for the orbits is shown in Table 3, in which the first and second numbers of the resonance represent the number of orbits completed by the smaller asteroid compared with the number of orbits completed by the spacecraft before a possible second encounter. See details in [35]. Only the more interesting orbits are shown, so there are some missing orbits in the results. As already explained, the present research focuses on studying the effects of the errors in the masses of the two smaller bodies in the trajectories found in [35]. Details on how to obtain the reference trajectories are omitted here, because it was already explained in detail in [35].

After the initial conditions of the resonant orbit were found, we removed the ones ending in collisions or escapes from the system. Then, we numerically integrated the orbits that survived both tests and measured the length of time that the spacecraft remained below 5 km from the center of each body. Tables 4–6 show these observational times (in days) that the spacecraft remained near Alpha (R_1), Beta (R_2), and Gamma (R_3). It is divided into three families of orbits, depending on if the error of the mass of Beta, the largest satellite body of the system, is positive (Family 1), zero (Family 2), or negative (Family 3). The maximum simulation time is always 62.50 days.

Table 4 shows the first family of orbits simulated, the ones in which there are positive errors in the mass of Beta. Table 5 shows the second family of orbits found, the ones in which there are no errors in the mass of Beta. Finally, Table 6 has the third family of orbits, which are the ones in which there are negative errors in the mass of Beta. The results show clearly that the errors in the masses of the asteroids affect the observational times, and it is necessary to take this fact into account to design the orbits, in particular the first ones,

when the spacecraft is arriving in the system. Which orbit should be used depends on the priorities and the specific goals of the mission. The important fact is to choose an orbit that has at least some observational times for all three bodies of the system. If there is a particular reason to give more importance to any of the bodies, this fact should be taken into account when selecting the orbits. It means that the results presented here give a large number of choices for the mission designers. Next, we show some good options for orbits as examples, not considering the specific aspects that a real mission may have.

Table 3. Nomenclature of the orbits. The text in bold separate the types of orbits.

Orbits with the Spacecraft Starting in the Periapsis (Same Side Orbits)
-2: Orbit internal to Gamma in resonance 3:4 -3: Orbit internal to Gamma in resonance 4:5 -4: Orbit external to Gamma in resonance 3:1
Orbits with the spacecraft starting in the apoapsis (same side orbits)
-5: Orbit internal to Beta in resonance 1:2 -12: Orbit external to Gamma in resonance 4:3 -15: Orbit external to Gamma in resonance 7:5
Orbit with the spacecraft starting in the periapsis (opposite side orbits)
-18: Orbit internal to Gamma in resonance 5:6
Orbit with the spacecraft starting in the apoapsis (opposite side orbits)
-20: Orbit external to Gamma in resonance 6:5
Orbit with the spacecraft starting in the periapsis (same side orbits with i = 13.87°)
-22: Orbit internal to Gamma in resonance 3:4
Orbits with the spacecraft starting in the apoapsis (same side orbits with i = 13.87°)
-25: Orbit internal to Beta in resonance 1:2 -27: Orbit internal to Beta in resonance 3:5 -31: Orbit external to Gamma in resonance 7:2
Orbit with the spacecraft starting in the periapsis (same side orbits with i = 90°)
-38: Orbit internal to Gamma in resonance 3:4
Orbit with the spacecraft starting in the apoapsis (same side orbits with i = 90°)
-42: Orbit internal to Beta in resonance 2:3 -52: Orbit external to Gamma in resonance 8:5
Orbits with the spacecraft starting in the apoapsis (same side orbits with i = 180°)
-59: Orbit internal to Beta in resonance 3:5 -60: Orbit internal to Beta in resonance 4:7 -61: Orbit internal to Beta in resonance 5:9

Table 4. First family of orbits simulated.

Family 1—Positive Errors in the Mass of Beta						
	Observation Times (Days)					
	Positive Errors in the Mass of Gamma		**No Errors in the Mass of Gamma**		**Negative Errors in the Mass of Gamma**	
Orbit	**True Anomaly 0°**	**True Anomaly 180°**	**True Anomaly 0°**	**True Anomaly 180°**	**True Anomaly 0°**	**True Anomaly 180°**
2						
R_1	6.95	9.62	18.57	18.57	10.23	10.23
R_2	0	0	0	0	0	0
R_3	5.88	8.47	13.20	13.20	6.98	6.98

Table 4. *Cont.*

Family 1—Positive Errors in the Mass of Beta						
	Observation Times (Days)					
	Positive Errors in the Mass of Gamma		No Errors in the Mass of Gamma		Negative Errors in the Mass of Gamma	
Orbit	True Anomaly 0°	True Anomaly 180°	True Anomaly 0°	True Anomaly 180°	True Anomaly 0°	True Anomaly 180°
3						
R_1	3.53	6.72	62.50	62.50	10.44	14.76
R_2	1.49	0.84	0	0	0	0
R_3	7.21	5.67	43.07	43.06	8.06	12.72
4						
R_1	6.50	6.48	4.94	6.02	13.34	4.72
R_2	0	0	0	1.36	0	0.62
R_3	7.87	5.62	6.74	6.99	15.84	5.93
5						
R_1	0	0	0	0	0	0
R_2	62.50	62.50	62.50	62.50	62.50	62.50
R_3	0	0	0	0	0	0
12						
R_1	3.55	3.61	25.86	25.87	12.62	16.51
R_2	0	0	0	0	0	0
R_3	4.65	4.96	30.07	30.07	13.85	18.22
15						
R_1	6.34	7.19	18.65	15.36	6.16	13.41
R_2	0	0	0	0	0	0
R_3	6.64	5.60	21.73	18.28	6.70	9.60
18						
R_1	28.54	25.41	11.83	12.44	20.68	17.55
R_2	0.87	0	0	0	0	0
R_3	9.25	8.46	8.13	8.45	17.10	11.56
20						
R_1	52.40	52.41	51.78	51.71	14.55	14.55
R_2	0	0	0	0	0	0
R_3	12.77	12.76	15.32	15.36	5.51	5.50
22						
R_1	1.86	1.86	62.50	62.50	6.03	6.03
R_2	0	0	0	0	0	0
R_3	1.45	1.45	43.31	43.33	4.04	4.04
25						
R_1	0	0	7.50	1.65	0.09	0
R_2	1.84	1.84	2.65	2.66	2.48	2.77
R_3	0	0	7.71	0.46	0.41	0.48
27						
R_1	10.56	7.06	1.87	13.37	11.29	1.66
R_2	1.48	4.33	2.65	1.75	2.21	5.65
R_3	9.93	7.94	2.79	14.84	11.85	2.55
31						
R_1	0	0	0	1.33	0.09	0.09
R_2	2.01	2.01	6.68	6.32	1.92	1.92
R_3	3.16	3.17	1.33	2.35	1.21	1.21

Table 4. *Cont.*

Family 1—Positive Errors in the Mass of Beta						
	Observation Times (Days)					
	Positive Errors in the Mass of Gamma		No Errors in the Mass of Gamma		Negative Errors in the Mass of Gamma	
Orbit	**True Anomaly 0°**	**True Anomaly 180°**	**True Anomaly 0°**	**True Anomaly 180°**	**True Anomaly 0°**	**True Anomaly 180°**
38						
R_1	5.78	5.78	7.07	7.07	6.32	6.32
R_2	0	0	0	0	0	0
R_3	2.64	2.64	3.23	3.23	3.36	3.36
42						
R_1	0.90	0.93	1.91	1.66	1.62	1.61
R_2	0.71	0.31	0.46	0.30	0.33	0.34
R_3	1.16	1.95	1.95	1.59	1.46	1.38
52						
R_1	8.09	11.34	12.86	13.03	14.36	12.06
R_2	0.78	0	0.49	0.47	0.16	0.43
R_3	6.94	9.56	10.41	10.08	10.78	9.79
59						
R_1	0.79	0.79	1.16	1.16	0.66	0.69
R_2	0.97	0.99	0.88	0.88	1.00	1.00
R_3	0.71	0.57	1.32	0.95	0.70	0.60
60						
R_1	0.11	0.11	0.10	0.10	0.09	0.09
R_2	0.17	0.17	0.16	0.16	0.17	0.17
R_3	0.24	0.24	0.24	0.24	0.24	0.24
61						
R_1	0.14	0.14	0.14	0.14	0.13	0.13
R_2	0.16	0.16	0.16	0.16	0.16	0.16
R_3	0.24	0.24	0.24	0.24	0.24	0.24

Table 5. Second family of orbits simulated.

Family 2—No Errors in the Mass of Beta						
	Observation Times (Days)					
	Positive Errors in the Mass of Gamma		No Errors in the Mass of Gamma		Negative Errors in the Mass of Gamma	
Orbit	**True Anomaly 0°**	**True Anomaly 180°**	**True Anomaly 0°**	**True Anomaly 180°**	**True Anomaly 0°**	**True Anomaly 180°**
2						
R_1	3.52	2.91	25.13	40.69	10.22	10.22
R_2	0	0	0	0	0	0
R_3	3.75	3.02	18.50	25.02	6.97	6.97
3						
R_1	3.42	3.41	62.50	62.50	4.43	4.43
R_2	0	0	0	0	0	0
R_3	3.51	3.22	43.07	43.07	2.66	2.66

Table 5. *Cont.*

Family 2—No Errors in the Mass of Beta						
	Observation Times (Days)					
	Positive Errors in the Mass of Gamma		No Errors in the Mass of Gamma		Negative Errors in the Mass of Gamma	
Orbit	**True Anomaly 0°**	**True Anomaly 180°**	**True Anomaly 0°**	**True Anomaly 180°**	**True Anomaly 0°**	**True Anomaly 180°**
4						
R_1	21.18	6.60	6.86	18.00	1.53	1.53
R_2	0	0	0	0	2.27	2.63
R_3	20.63	7.60	5.92	20.61	1.98	1.98
5						
R_1	0	0	0	0	0	0
R_2	62.50	62.50	62.50	62.50	62.50	62.50
R_3	0	0	0	0	0	0
12						
R_1	2.74	3.02	25.83	25.82	7.26	8.80
R_2	0	1.14	0	0	0	0
R_3	4.67	5.04	30.39	30.40	7.05	8.59
15						
R_1	5.96	9.52	24.27	24.26	11.90	42.46
R_2	0	0	0	0	0.24	0
R_3	5.03	7.56	27.15	27.15	12.79	31.33
18						
R_1	9.66	12.08	35.73	11.36	6.19	6.19
R_2	0	0	0.69	0	0	0
R_3	5.36	5.83	16.51	5.99	2.64	2.64
20						
R_1	52.19	52.20	36.18	35.00	32.56	24.10
R_2	0	0	0.43	0	0	0
R_3	12.33	12.32	12.61	11.63	12.65	12.39
22						
R_1	1.86	1.86	62.50	62.50	6.03	6.03
R_2	0	0	0	0	0	0
R_3	1.46	1.46	43.03	43.02	4.06	4.05
25						
R_1	2.71	2.73	6.86	2.40	2.36	2.33
R_2	1.42	0.99	0.88	0	0.55	0.55
R_3	1.48	1.43	7.58	1.71	1.25	2.68
27						
R_1	0	0	5.51	5.64	0	0
R_2	2.22	2.20	4.58	4.55	2.32	2.32
R_3	0.51	0.50	4.27	5.06	0.32	0.32
31						
R_1	4.55	10.91	4.32	5.39	1.62	11.24
R_2	5.80	1.15	1.59	2.23	4.48	1.38
R_3	5.08	8.69	5.17	5.65	3.31	11.43

Table 5. *Cont.*

Family 2—No Errors in the Mass of Beta						
	Observation Times (Days)					
	Positive Errors in the Mass of Gamma		No Errors in the Mass of Gamma		Negative Errors in the Mass of Gamma	
Orbit	**True Anomaly 0°**	**True Anomaly 180°**	**True Anomaly 0°**	**True Anomaly 180°**	**True Anomaly 0°**	**True Anomaly 180°**
38						
R_1	6.61	6.61	8.12	8.13	6.71	6.71
R_2	0	0	0.32	0.37	0	0
R_3	3.05	3.05	4.43	4.40	3.81	3.80
42						
R_1	1.87	1.87	2.16	2.18	1.88	1.88
R_2	0.69	0.69	0.34	0.34	0.78	0.78
R_3	1.06	1.04	0.88	1.01	1.34	1.34
52						
R_1	6.53	5.57	9.15	5.00	13.73	11.90
R_2	0.34	0.44	0	0	0	0.31
R_3	4.57	4.31	8.23	4.03	9.84	9.57
59						
R_1	2.39	2.39	1.88	1.86	2.14	2.14
R_2	2.55	2.56	2.68	2.68	2.89	2.93
R_3	2.83	2.83	2.62	2.61	3.57	3.55
60						
R_1	2.65	2.67	2.27	1.65	0.69	0.69
R_2	1.01	0.64	1.53	1.07	0.35	0.35
R_3	2.08	1.97	2.35	1.34	0.54	0.54
61						
R_1	0.69	0.80	2.48	2.52	0.15	0.15
R_2	2.58	2.66	1.39	1.33	0.17	0.17
R_3	2.79	2.75	1.52	1.90	0.25	0.25

Table 6. Third family of orbits simulated.

Family 3—Negative Errors in the Mass of Beta						
	Observation Times (Days)					
	Positive Errors in the Mass of Gamma		No Errors in the Mass of Gamma		Negative Errors in the Mass of Gamma	
Orbit	**True Anomaly 0°**	**True Anomaly 180°**	**True Anomaly 0°**	**True Anomaly 180°**	**True Anomaly 0°**	**True Anomaly 180°**
2						
R_1	2.85	2.98	18.55	18.55	10.22	10.22
R_2	0.65	0.72	0	0	0	0
R_3	2.46	2.49	13.17	13.17	6.97	6.96
3						
R_1	5.59	3.82	62.50	62.50	4.42	4.41
R_2	1.44	0	0	0	0	0
R_3	5.61	3.95	43.06	43.07	2.65	2.64

Table 6. *Cont.*

Family 3—Negative Errors in the Mass of Beta						
	Observation Times (Days)					
	Positive Errors in the Mass of Gamma		No Errors in the Mass of Gamma		Negative Errors in the Mass of Gamma	
Orbit	**True Anomaly 0°**	**True Anomaly 180°**	**True Anomaly 0°**	**True Anomaly 180°**	**True Anomaly 0°**	**True Anomaly 180°**
4						
R_1	2.59	24.33	22.45	3.60	5.97	4.85
R_2	0	0	0	0.68	0.51	0.57
R_3	3.10	23.88	22.49	5.25	5.53	5.24
5						
R_1	0	0	0	0	0	0
R_2	62.50	62.50	62.50	62.50	62.50	62.50
R_3	0	0	0	0	0	0
12						
R_1	1.97	3.05	25.80	25.78	22.53	4.16
R_2	0.49	0.49	0	0	0	1.65
R_3	3.22	5.37	30.39	30.37	23.71	5.23
15						
R_1	3.84	3.84	23.95	23.95	18.00	17.38
R_2	0	0	0	0	0	0
R_3	4.08	4.08	26.53	26.53	17.25	17.99
18						
R_1	7.27	6.48	10.67	27.67	45.54	9.66
R_2	0	0	0.24	0	0	0
R_3	3.76	2.98	5.98	18.11	20.09	5.58
20						
R_1	52.27	52.27	51.56	51.57	52.55	51.72
R_2	0	0	0	0	0	0
R_3	12.79	12.80	14.95	14.95	17.37	18.03
22						
R_1	1.86	1.86	62.50	62.50	6.02	6.02
R_2	0	0	0	0	0	0
R_3	1.46	1.46	42.82	42.83	4.10	4.09
25						
R_1	0.39	0.75	1.87	2.21	0.99	1.04
R_2	1.60	1.89	0.62	0.45	2.44	2.47
R_3	1.89	1.95	2.55	2.28	1.65	1.66
27						
R_1	0	0	0	0	0	0
R_2	1.68	2.11	1.62	1.62	1.34	1.34
R_3	0.43	0.43	0.36	0.36	0.35	0.35
31						
R_1	0.99	2.45	7.28	6.89	7.26	7.26
R_2	0.57	2.12	2.13	4.45	1.40	1.40
R_3	1.60	2.33	5.30	5.31	4.40	4.40

Table 6. *Cont.*

Family 3—Negative Errors in the Mass of Beta						
	Observation Times (Days)					
	Positive Errors in the Mass of Gamma		No Errors in the Mass of Gamma		Negative Errors in the Mass of Gamma	
Orbit	**True Anomaly 0°**	**True Anomaly 180°**	**True Anomaly 0°**	**True Anomaly 180°**	**True Anomaly 0°**	**True Anomaly 180°**
38						
R_1	7.97	7.97	8.49	8.27	8.14	8.14
R_2	0	0	0.09	0	0	0
R_3	4.38	4.38	4.27	4.02	5.02	5.03
42						
R_1	1.79	1.78	2.20	2.42	1.58	1.58
R_2	1.45	1.44	0.69	0.52	0.03	0.04
R_3	0.70	0.85	1.01	0.94	0.11	0.11
52						
R_1	1.81	1.81	7.33	5.76	18.28	18.36
R_2	0	0	0	0	0	0
R_3	1.68	1.68	7.53	5.46	13.27	13.98
59						
R_1	0.78	0.77	0.31	0.31	0.25	0.25
R_2	3.05	3.05	2.84	2.84	2.68	2.68
R_3	2.96	2.97	2.93	2.93	2.76	2.76
60						
R_1	3.11	3.21	3.11	3.02	2.65	2.64
R_2	2.97	2.82	2.99	2.92	3.13	3.14
R_3	2.85	2.99	3.17	3.11	2.99	2.99
61						
R_1	3.14	3.15	2.55	2.51	2.82	2.82
R_2	1.62	1.48	1.61	1.71	2.09	2.08
R_3	2.80	2.86	2.41	2.40	2.40	2.58

5.1. A Good Option to Observe Alpha and Gamma

Several options are available to observe the bodies Alpha and Gamma. As an example, Orbit 20 is a good choice, with some observational times in all the scenarios simulated. The observational times of all scenarios considering the asteroid in its periapsis and in its apoapsis at the initial time can be seen in Table 7. Note that, in the nominal case (0) (0), when the asteroid is located at its periapsis, the spacecraft stays 36.18 days near Alpha and 12.61 days near Gamma. The values are different for each scenario, but there are at least 14.55 days to observe Alpha and 5.50 days to observe Gamma in the worst scenario, which is the situation in which there is a positive error in the mass of Beta and a negative error in the mass of Gamma, when the asteroid is in its apoapsis. The orbits with the spacecraft starting at its periapsis are very similar. The other observational times are all above these limits. The largest observation time for the bodies occurs in two different situations: when the asteroid starts at its periapsis and the vehicle observes Alpha for 52.55 days; and when the asteroid starts in its apoapsis and the vehicle observes Gamma for 18.03 days. Both situations happen when the errors of the Beta and Gamma masses are negative.

Figure 3 shows the trajectories of the spacecraft and the secondary bodies in all the scenarios described. The simulation time is always 62.50 days. In most scenarios, the simulations last the whole time used for the numerical integration, and the orbits of the vehicle are more concentrated around Alpha and Gamma. Note that, in scenario A, the

vehicle collides with the main body and the integration stops in 51.40 days. In scenario C, the integration lasts for 17.70 days and the spacecraft collides with Gamma. The vehicle also collides with Gamma in scenario F and the simulation lasts 41.67 days. It is noted that the trajectory related to the nominal situation A is different from the others, because the spacecraft reaches and crosses the orbit of Beta around Alpha. All the error scenarios make the trajectory to be closer to Alpha, resulting in more confined trajectories.

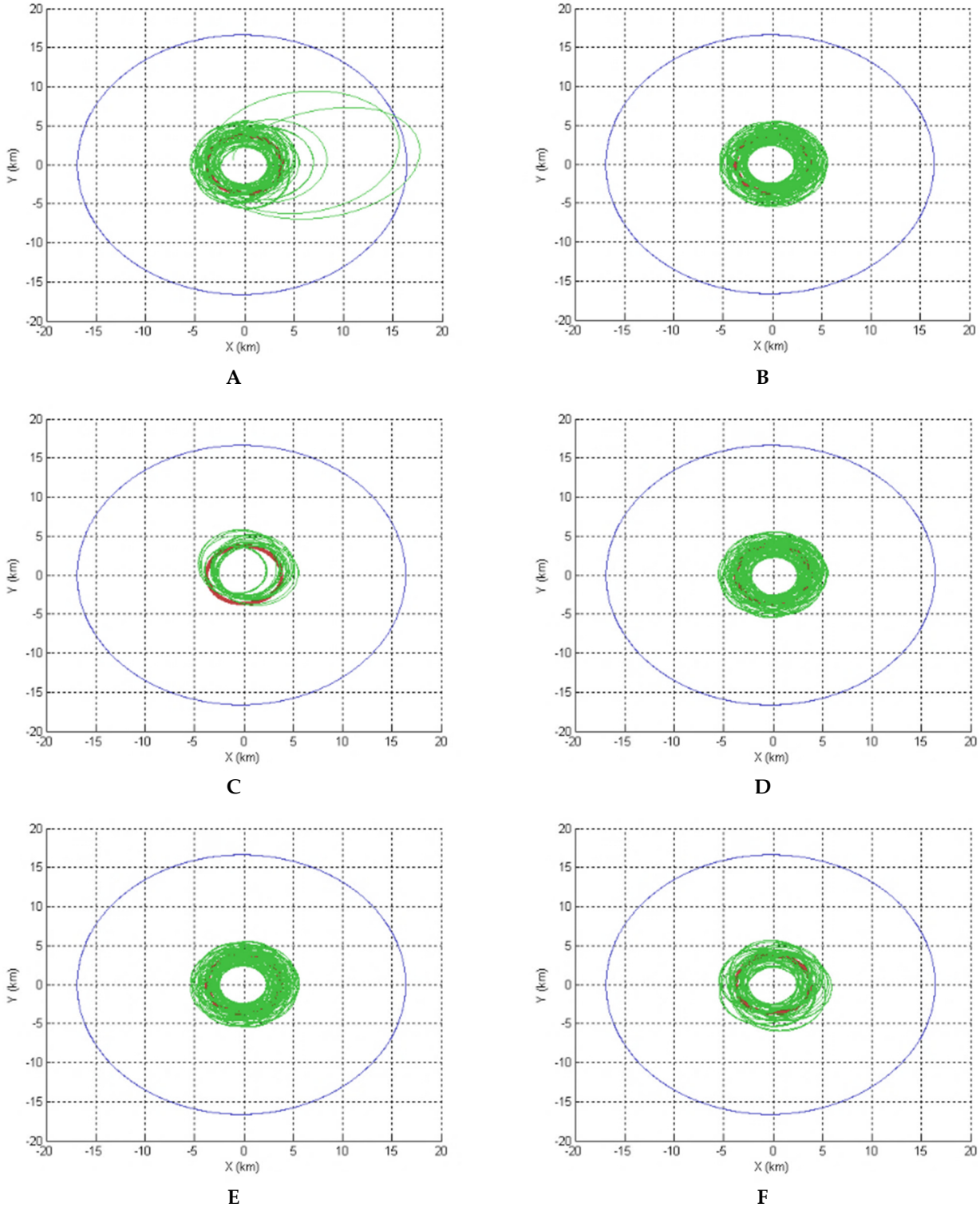

Figure 3. *Cont.*

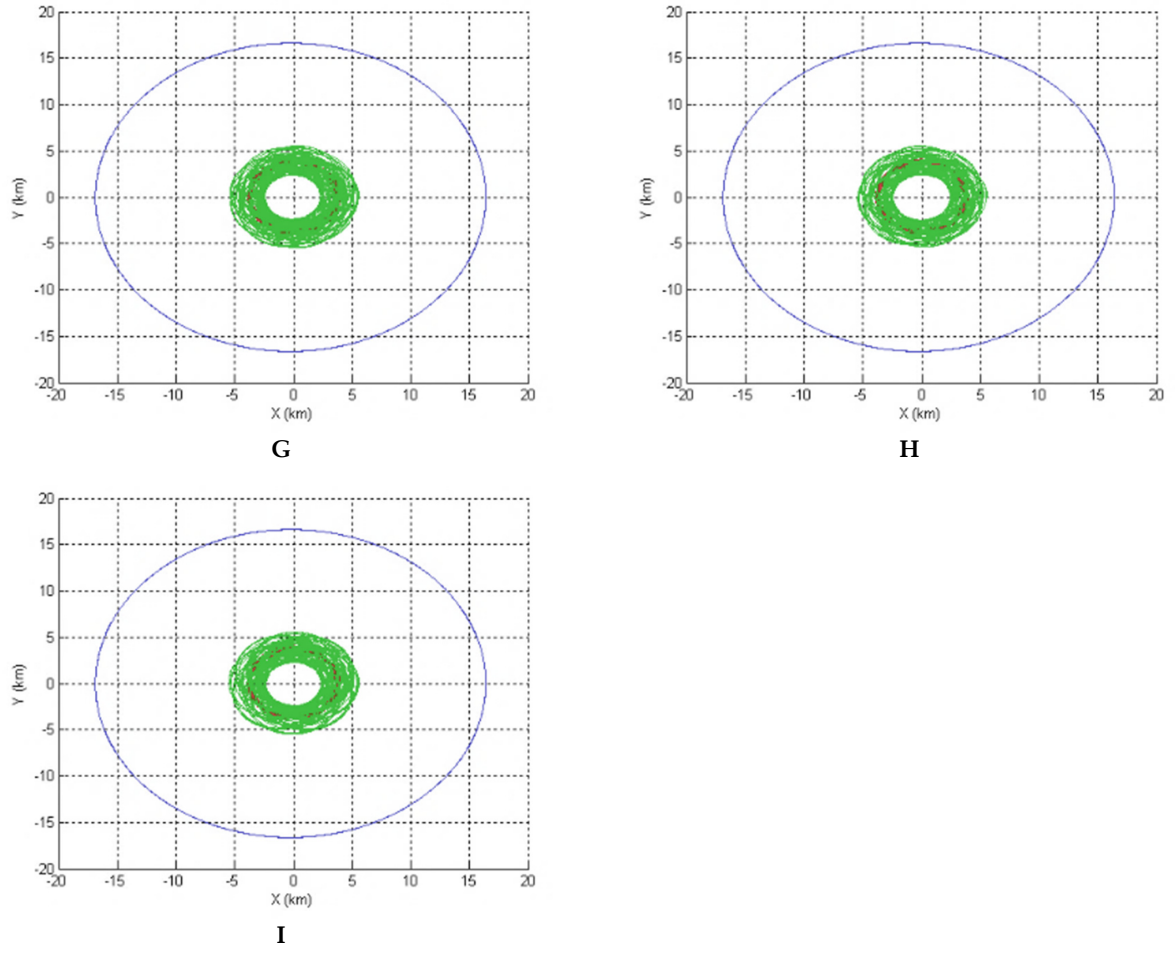

Figure 3. Trajectory of the spacecraft (green), Beta (blue), and Gamma (red) for Orbit 20 when the spacecraft starts its motion in the periapsis in all scenarios ((**A**): nominal value, (**B**): (+) (+), (**C**): (+) (−), (**D**): (+) (0), (**E**): (0) (+), (**F**): (0) (−), (**G**): (−) (+), (**H**): (−) (−), and (**I**): (−) (0)).

Table 7. Observation times for the nine scenarios for Orbit 20. $R_2 = 0$.

Scenario		Observational Times (Days)	
		True Anomaly 0°	True Anomaly 180°
(+) (+)	R_1	52.40	52.41
	R_3	12.77	12.76
(+) (0)	R_1	51.78	51.71
	R_3	15.32	15.36
(+) (−)	R_1	14.55	14.55
	R_3	5.51	5.50
(0) (+)	R_1	52.19	52.20
	R_3	12.33	12.32
(0) (0)	R_1	36.18	35.00
	R_3	12.61	11.63
(0) (−)	R_1	32.56	24.10
	R_3	12.65	12.39
(−) (+)	R_1	52.27	52.27
	R_3	12.79	12.80
(−) (0)	R_1	51.56	51.57
	R_3	14.95	14.95
(−) (−)	R_1	52.55	51.72
	R_3	17.37	18.03

5.2. A Good Option to Observe Beta

Orbit 5 is an interesting option to observe Beta. It has the same observation times in all scenarios simulated, which means that even the potential errors in the mass of Beta do not change this characteristic of the orbit. In the nominal case, the spacecraft does not observe Alpha and Gamma, but remains all 62.50 days of its integration time around Beta. This can be observed in all scenarios simulated. Figure 4 shows the trajectory of the spacecraft and the secondary bodies of the system for the nominal case. It is very similar to the other scenarios, so the figures are omitted here.

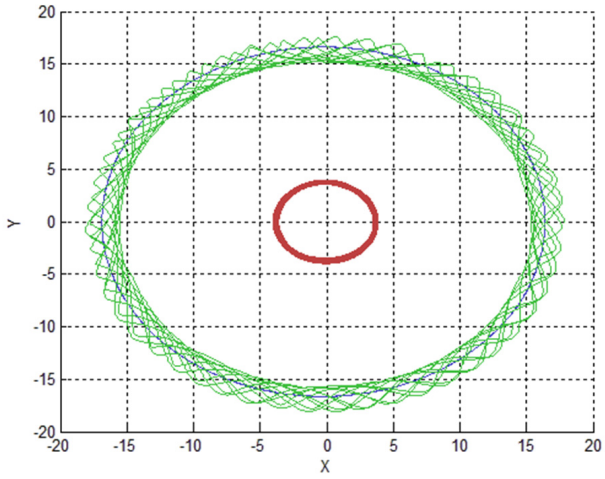

Figure 4. Trajectory of the spacecraft (green), Beta (blue), and Gamma (red) for Orbit 5 in the nominal case (similar to the other scenarios).

5.3. An Option to Observe All the Three Bodies of the System

Orbits to observe the three bodies of the system are not very common, but they are very important. A good choice is Orbit 59, where the asteroid starts at its periapsis, in the nominal case (0) (0). The spacecraft remains 1.88 days close to Alpha, 2.68 days close to Beta, and 2.62 days observing Gamma. Table 8 shows the observational times of all the possible scenarios for Orbit 59, both considering the asteroid in its periapsis and its apoapsis. In the worst scenario, when the errors in the masses of Beta and Gamma are negative and the asteroid starts its motion at its periapsis, the observational times are 0.25 days for Alpha, 2.68 days for Beta, and 2.76 days for Gamma, which is still enough to obtain a better evaluation of the real masses of the three bodies. In the best scenario, when there is no error in the mass of Beta and the error in the mass of Gamma is negative, and the asteroid is in its apoapsis, the observational times are 2.14 days for Alpha, 2.93 days for Beta, and 3.55 days for Gamma. It is important to remember that those times were calculated using the definition of 5 km from the center of the body to be considered an observation time, but there are also times when the spacecraft remains in the range of 5–10 km, which is still useful for some observations.

Figure 5 shows the trajectories of the spacecraft and the secondary bodies for this orbit. The simulation time in the situations above is 62.50 days. It is observed that the trajectories have noticeable differences for different scenarios. In all scenarios, the integration lasted the total integration time, with the exception of scenario B, which lasted 27.34 days after a collision with the main body. It is clear that the errors in the masses modify the trajectories, not only the observational times. Scenarios E, G, and H have orbits that are less disturbed ellipses. Scenarios F and I have ellipses with faster advances in the periapsis. Scenarios C and D present orbits with higher apoapsis.

Table 8. Observation times for the eight scenarios with errors for Orbit 59. True Anomaly 0° is on the left and True Anomaly 180° is on the right. For the nominal case ((0) (0)), we have $R_1 = 1.88$, $R_2 = 2.68$, $R_3 = 2.62$ for True Anomaly 0°, and $R_1 = 1.86$, $R_2 = 2.68$, $R_3 = 2.61$ for True Anomaly 180°.

Scenario **(+) (+)**	R_1	0.79	0.79
	R_2	0.97	0.99
	R_3	0.71	0.57
Scenario **(+) (0)**	R_1	1.16	1.16
	R_2	0.88	0.88
	R_3	1.32	0.95
Scenario **(+) (−)**	R_1	0.66	0.69
	R_2	1.00	1.00
	R_3	0.70	0.60
Scenario **(0) (+)**	R_1	2.39	2.39
	R_2	2.55	2.56
	R_3	2.83	2.83
Scenario **(0) (−)**	R_1	2.14	2.14
	R_2	2.89	2.93
	R_3	3.57	3.55
Scenario **(−) (+)**	R_1	0.78	0.77
	R_2	3.05	3.05
	R_3	2.96	2.97
Scenario **(−) (0)**	R_1	0.31	0.31
	R_2	2.84	2.84
	R_3	2.93	2.93
Scenario **(−) (−)**	R_1	0.25	0.25
	R_2	2.68	2.68
	R_3	2.76	2.76

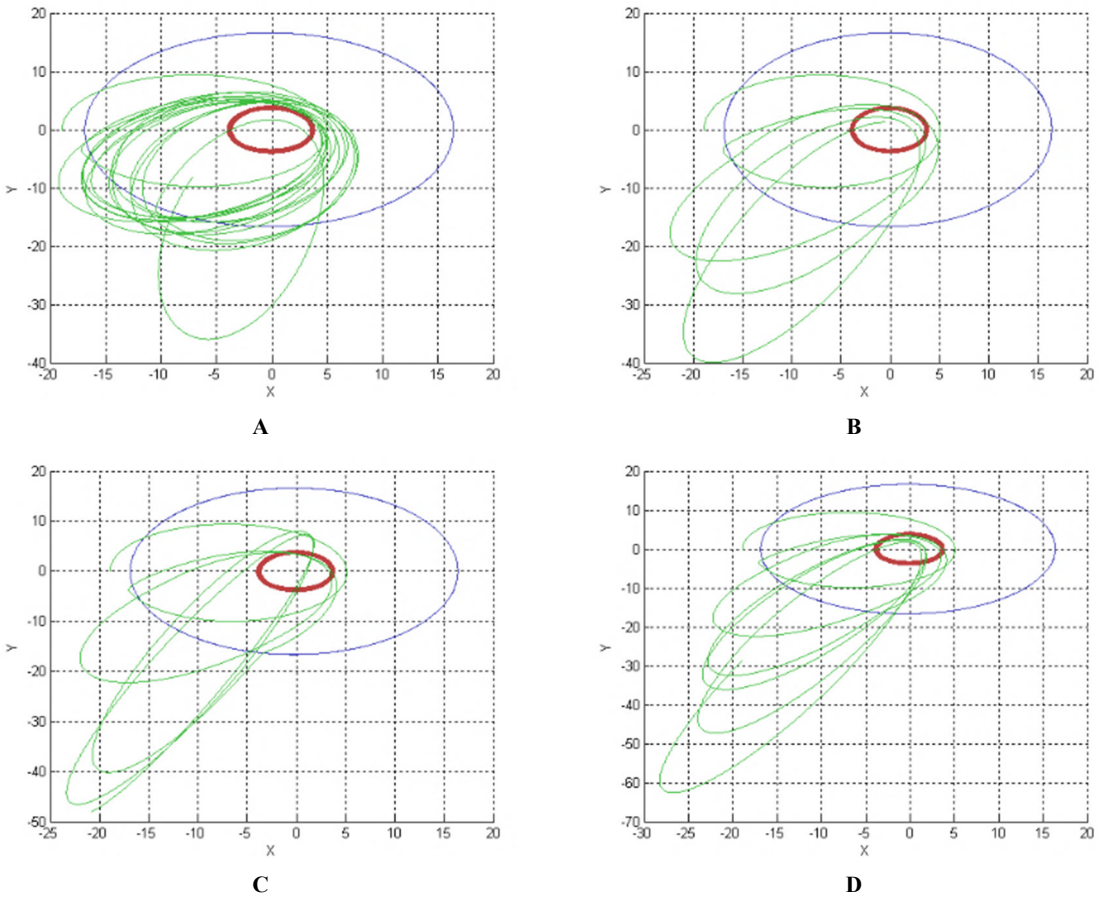

Figure 5. *Cont.*

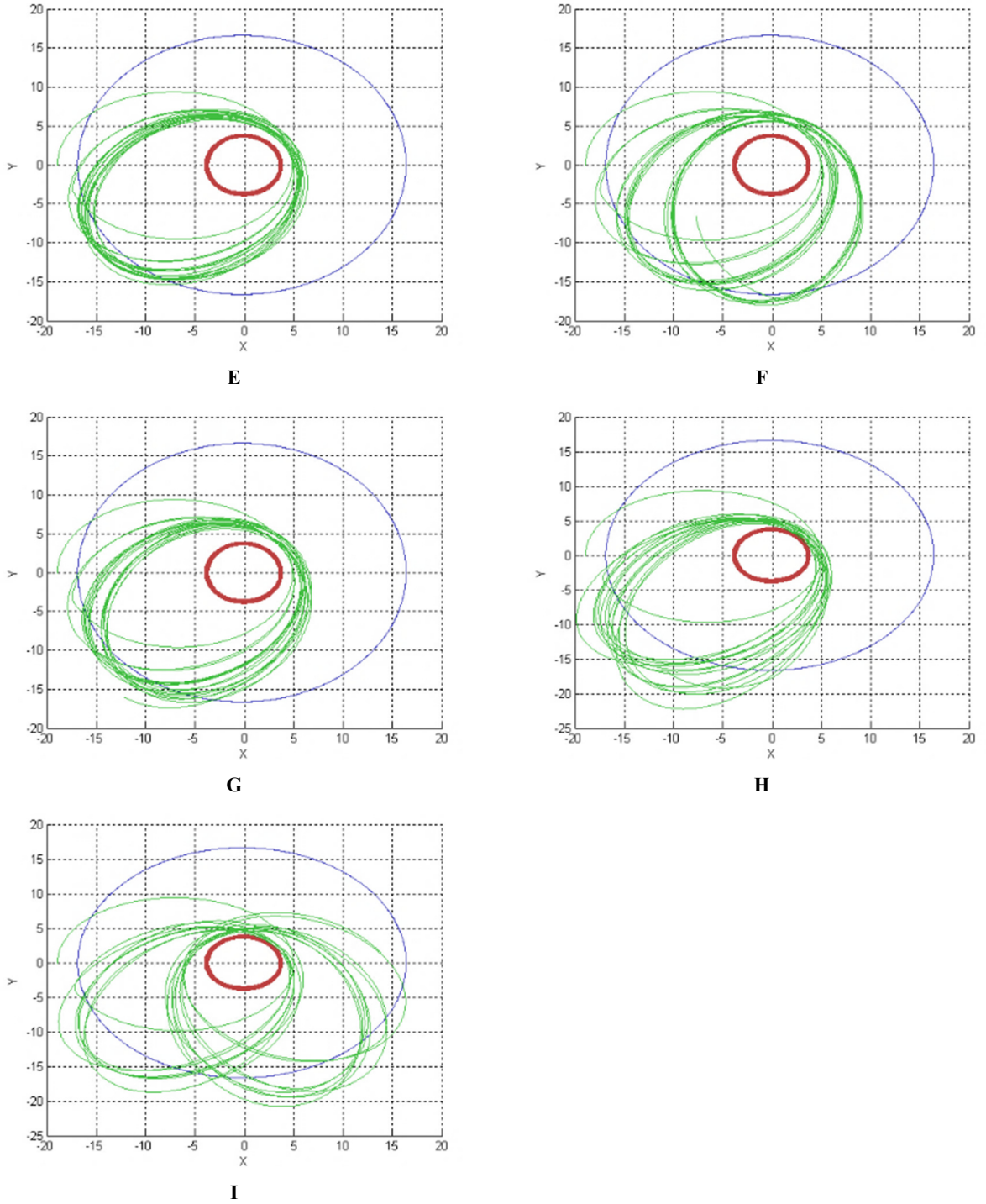

Figure 5. Trajectories of the spacecraft (green), Beta (blue), and Gamma (red) for orbit 59 with the spacecraft starting in the periapsis in all scenarios ((**A**): nominal value, (**B**): (+) (+), (**C**): (+) (−), (**D**): (+) (0), (**E**): (0) (+), (**F**): (0) (−), (**G**): (−) (+), (**H**): (−) (−) and (**I**): (−) (0)).

6. Conclusions

The present research studied the effects of the errors in the masses of the smaller bodies Beta and Gamma of the triple system $2001SN_{263}$ in the observational times that a spacecraft may have when orbiting this system. The time-histories of the relative distances between the spacecraft and all three asteroids of the 2001SN263 system are measured. The orbits that spend more time close to each one of the asteroids can be selected through the data that come from the simulations. Nine error scenarios were simulated, to take into account

the possibilities of negative, zero, or positive errors in the masses of Beta and Gamma. The mass of Alpha is assumed to be accurately known when compared to the errors of the smaller asteroids. This assumption is justified because there is more information available about this larger body. The most important contribution to the mission designer is to find orbits that have some observational times for all the nine errors scenarios considered, which is important considering the fact that the smaller bodies are poorly observed.

The results showed the existence of several orbits that satisfy this condition. Orbit 20 is an example of an orbit that is useful to observe Alpha and Gamma. The minimum observation time regarding Alpha is 14.55 days and the maximum is 52.55 days. Gamma is observed between 5.50 days and 18.03 days. Note that, in this orbit, the nominal case was the one that presented the longest observation time. If the goal is to only observe Beta, Orbit 5 is recommended. During the simulations, the spacecraft remained around Beta at all times.

Finally, in Orbit 59, it is observed that the spacecraft remains between 0.25 days and 2.14 days near Alpha; 0.88 days and 2.93 days around Beta; and 0.70 and 3.55 days observing Gamma. It means that it is possible to find orbits that have observational times for all the scenarios simulated, and those orbits are very important to place the spacecraft at the beginning of the mission, before a better estimation of the masses is made.

Author Contributions: Conceptualization, Formal analysis, Funding acquisition, Investigation, Methodology, Validation, Visualization, Writing—original draft, and Writing—review & editing: A.K.d.A.J., B.Y.P.M.M., A.P.M.C., V.M.G. and A.F.B.d.A.P. All authors have read and agreed to the published version of the manuscript.

Funding: The authors would like to thank several institutions for their support: grants # 2018/07377-6 and 2016/24561-0 from São Paulo Research Foundation (FAPESP); grants # 309089/2021-2 and 432513/2018-3 from the National Council for Scientific and Technological Development (CNPq); and financial support from the National Council for the Improvement of Higher Education (CAPES). This paper has been supported by the RUDN University Strategic Academic Leadership Program.

Acknowledgments: We thank the comments and suggestions of the referees.

Conflicts of Interest: The authors declare no conflict of interest.

References

1. Belton, M.J.S.; Veverka, J.; Thomas, P.; Helfenstein, P.; Simonelli, D.; Chapman, C.; Davies, M.E.; Greeley, R.; Greenberg, R.; Head, J.; et al. Galileo Encounter with 951 Gaspra: First pictures of an asteroid. *Science* **1992**, *257*, 1647. [CrossRef] [PubMed]
2. Belton, M.J.; Chapman, C.R.; Klaasen, K.P.; Harch, A.P.; Thomas, P.C.; Veverka, J.; McEwen, A.S.; Pappalardo, R.T. Galileo's Encounter with 243 Ida: Overview of the imaging experiment. *Icarus* **1996**, *120*, 1–19. [CrossRef]
3. Binzel, R.P.; Rivkin, A.; Bus, S.J.; Sunshine, J.; Burbine, T.H. MUSES-C target asteroid (25143) 1998 SF36: A reddened ordinary chondrite. *Meteorit. Planet. Sci.* **2001**, *36*, 1167–1172. [CrossRef]
4. Veverka, J.; Farquhar, B.B.; Robinson, M.J.; Thomas, P.C.; Murchie, S.; Harch, A.P.; Antreasian, P.G.; Chesley, S.R.; Miller, J.K.; Owen, W.M.; et al. The landing of the Near-Shoemaker spacecraft on asteroid 433 Eros. *Nature* **2001**, *413*, 390–393. [CrossRef]
5. Miller, J.K.; Konopliv, A.S.; Antreasian, P.G.; Bordi, J.J.; Chesley, S.; Helfrich, C.E.; Owen, W.M.; Wang, T.C.; Williams, B.G.; Yeomans, D.K.; et al. Determination of shape, gravity and rotational state of asteroid 433 Eros. *Icarus* **2002**, *155*, 3–17. [CrossRef]
6. Broschart, S.B.; Scheeres, D.J. Control of hovering spacecraft near small bodies: Application to asteroid 25143 Itokawa. *J. Guid. Control Dyn.* **2005**, *28*, 343–354. [CrossRef]
7. Huntress, W.; Stetson, D.; Farquhar, R.; Zimmerman, J.; Clark, B.; O'Neil, W.; Bourke, R.; Foing, B. The next steps in exploring deep space—A cosmic study by the IAA. *Acta Astronaut.* **2006**, *58*, 304–377. [CrossRef]
8. Yoshikawa, M.; Fujiwara, A.; Kawaguchi, J. Hayabusa and its adventure around the tiny asteroid Itokawa. *Proc. Int. Astron. Union* **2006**, *2*, 323–324. [CrossRef]
9. Brum, A.G.V.D.; Hetem, A., Jr.; Rêgo, I.D.S.; Francisco, C.P.F.; Fenili, A.; Madeira, F.; Da Cruz, F.C.; Assafin, M. Preliminary development plan of the ALR, the laser rangefinder for the Aster deep space mission to the 2001 SN263 asteroid. *J. Aerosp. Tehchnol. Manag.* **2011**, *3*, 331–338. [CrossRef]
10. Jones, T.; Bellerose, J.; Lee, P.; Prettyman, T.; Lawrence, D.; Smith, P.; Gaffey, M.; Nolan, M.; Goldsten, J.; Thomas, P.; et al. Amor: Investigating The Triple Asteroid System 2001 SN263. *AAS/Div. Planet. Sci. Meet. Abstr. #42* **2010**, *42*, 49. Available online: https://ui.adsabs.harvard.edu/abs/2010DPS....42.4929J (accessed on 23 August 2022).

11. Müller, T.G.; Ďurech, J.; Hasegawa, S.; Abe, M.; Kawakami, K.; Kasuga, T.; Kinoshita, D.; Kuroda, D.; Urakawa, S.; Okumura, S.; et al. Thermo-physical properties of 162173 (1999 JU3), a potential flyby and rendezvous target for interplanetary missions. *Astron. Astrophys.* **2011**, *525*, A145. [CrossRef]
12. Tardivel, S.; Michel, P.; Scheeres, D.J. Deployment of a lander on the binary asteroid (175706) 1996 FG3, potential target of the European MarcoPolo-R sample return mission. *Acta Astronaut.* **2013**, *89*, 60–70. [CrossRef]
13. Tsuda, Y.; Yoshikawa, M.; Abe, M.; Minamino, H.; Nakazawa, S. System design of the Hayabusa 2—Asteroid sample return mission to 199 JU3. *Acta Astronaut.* **2013**, *91*, 356–362. [CrossRef]
14. Chesley, S.R.; Farnocchia, D.; Nolan, M.C.; Vokrouhlický, D.; Chodas, P.W.; Milani, A.; Spoto, F.; Rozitis, B.; Benner, L.A.; Bottke, W.F.; et al. Orbit and bulk density of the OSIRIS-REx target Asteroid (101955) Bennu. *Icarus* **2014**, *235*, 5–22. [CrossRef]
15. Bottke, W.F.; Vokrouhlický, D.; Walsh, K.J.; Delbo, M.; Michel, P.; Lauretta, D.S.; Campins, H.; Connolly, H.C.; Scheeres, D.J.; Chelsey, S.R. In search of the source of asteroid (101955) Bennu: Applications of the stochastic YORP model. *Icarus* **2015**, *247*, 191–217. [CrossRef]
16. NASA. Available online: https://www.nasa.gov/osiris-rex (accessed on 25 April 2017).
17. Surovik, D.A.; Scheeres, D.J. Autonomous maneuver planning at small bodies via mission objective reachability analysis. In Proceedings of the 2014 AIAA/AAS Astrodynamics Specialist Conference, San Diego, CA, USA, 4–7 August 2014.
18. Werner, R.A. The gravitational potential of a homogeneous polyhedron or don't cut corners. *Celest. Mech. Dyn. Astron.* **1994**, *59*, 253–278. [CrossRef]
19. Scheeres, D.J. Dynamics about uniformly rotating triaxial ellipsoids: Application to asteroids. *Icarus* **1994**, *121*, 225–238. [CrossRef]
20. Scheeres, D.J. *Orbital Motion in Strongly Perturbed Environments*; Springer: Boulder, CO, USA, 2012; ISBN 978-3-642-03255-4.
21. Scheeres, D.J. Orbit mechanics about asteroids and comets. *J. Guid. Control Dyn.* **2012**, *35*, 987–997. [CrossRef]
22. Scheeres, D.J. Orbital mechanics about small bodies. *Acta Astronaut.* **2012**, *72*, 1–14. [CrossRef]
23. Rossi, A.; Marzari, F.; Farinella, P. Orbital evolution around irregular bodies. *Earth Planets Space* **1999**, *51*, 1173–1180. [CrossRef]
24. Scheeres, D.J.; Hu, W. Secular motion in a 2nd degree and order gravity field with no rotation. *Celest. Mech. Dyn. Astron.* **2001**, *79*, 183–200. [CrossRef]
25. Bartczakk, P.; Breiter, S.; Jusiel, P. Ellipsoids, material points and material segments. *Celest. Mech. Dyn. Astron.* **2006**, *96*, 31–48. [CrossRef]
26. Byram, S.M.; Scheeres, D.J. Stability of Sun-Synchronous Orbits in the Vicinity of a Comet. *J. Guid. Control Dyn.* **2009**, *32*, 1550–1559. [CrossRef]
27. Shang, H.; Wu, X.; Cui, P. Periodic orbits in the doubly synchronous binary asteroid systems and their applications in space missions. *Astrophys. Space Sci.* **2014**, *355*, 69–87. [CrossRef]
28. Yang, H.; Gong, S.; Baoyin, H. Two-impulse transfer orbits connecting equilibrium points of irregular-shaped asteroids. *Astrophys. Space Sci.* **2015**, *357*, 66. [CrossRef]
29. Zeng, X.; Baoyin, H.; Li, J. Updated Rotating Mass Dipole with Oblateness of One Primary (II): Out-of-plane Equilibria and Their Stability. *Astrophys. Space Sci.* **2016**, *361*, 15. [CrossRef]
30. Chanut, T.G.G.; Aljbaae, S.; Prado, A.F.B.A.; Carruba, V. Dynamics in the vicinity of (101955) Bennu: Solar radiation pressure effects in equatorial orbits. *Mon. Not. R. Astron. Soc.* **2017**, *470*, 2687–2701. [CrossRef]
31. Almeida, A.K., Jr.; Oliveira, G.M.C.; Prado, A.F.B.A. Artificial equilibrium points and bi-impulsive maneuvers to observe 243 Ida. *Chin. J. Aeronaut.* **2021**, *34*, 410. [CrossRef]
32. Araújo, R.A.N. O Sistema Triplo de Asteroides 2001SN263: Dinâmica Orbital e Estabilidade. Doctorate. Degree Thesis, INPE—National Institute for Space Research, São José dos Campos, Brazil, 2011.
33. Fang, J.; Margot, J.L.; Brozovic, M.; Nolan, M.C.; Benner, L.A.M.; Taylor, P.A. Orbits of near-earth asteroid triple 2001SN263 and 1994 CC: Properties, origin, and evolution. *Astron. J.* **2011**, *141*, 154. [CrossRef]
34. Araújo, R.A.N.; Winter, O.C.; Prado, A.F.B.A. Stable retrograde orbits around the triple system 2001 SN263. *Mon. Not. R. Astron. Soc.* **2015**, *449*, 4404. [CrossRef]
35. Masago, B.Y.P.L.; Prado, A.; Chiaradia, A.P.M.; Gomes, V.M. Developing the Precessing Inclined Bi-Elliptical Four-Body Problem with Radiation Pressure" to search for orbits in the triple asteroid 2001SN263. *Adv. Space Res.* **2016**, *57*, 962–982. [CrossRef]
36. Sanchez, D.M.; Prado, A.F.B.A. Searching for Less-Disturbed Orbital Regions Around the Near-Earth Asteroid 2001 SN263. *J. Spacecr. Rocket.* **2019**, *56*, 1775–1785. [CrossRef]
37. Cavalca, M.P.O.; Gomes, V.M.; Sanchez, D.M. Mid-range natural orbits around the triple asteroid 2001SN263. *Eur. Phys. J. Spéc. Top.* **2020**, *229*, 1557–1572. [CrossRef]
38. Valvano, G.; Winter, O.C.; Sfair, R.; Oliveira, R.M.; Borderes-Motta, G. 2001 SN263—The contribution of their irregular shapes on the neighbourhood dynamics. *Mon. Not. R. Astron. Soc.* **2022**, *515*, 606–616. [CrossRef]
39. Brum, A.G.V.D.; Schuindt, C.M. A Proposal of Optical Navigation for Deep Space Mission ASTER to Explore NEA 2001-SN263. *J. Aerosp. Technol. Manag.* **2022**, *14*. [CrossRef]
40. Deienno, R.; Sanchez, D.M.; de Almeida Prado, A.F.B.; Smirnov, G. Satellite de-orbiting via controlled solar radiation pressure. *Celest. Mech. Dyn. Astron.* **2016**, *126*, 433–459. [CrossRef]
41. Holman, M.J.; Wiegert, P.A. Long-term Stability of Planets in Binary Systems. *Astron. J.* **1999**, *117*, 621–628. [CrossRef]
42. Hu, W.; Scheeres, D.J. Numerical determination of stability regions for orbital motion in uniformly rotating second degree and order gravity fields. *Planet. Space Sci.* **2004**, *52*, 685–692. [CrossRef]

43. Mudryk, L.R.; Wu, Y. Resonance Overlap is Responsible for Ejecting Planets in Binary Systems. *Astrophys. J. Lett.* **2006**, *639*, 423–431. [CrossRef]
44. Nolan, M.C.; Howell, E.S.; Benner, L.A.M.; Ostro, S.J.; Giorgini, J.D.; Busch, M.W.; Carter, L.M.; Anderson, R.F.; Magri, C.; Campbell, D.B.; et al. Arecibo Radar Imaging of 2001SN263: A near-Earth triple asteroid system. *Asteroids Comets Meteors* **2008**, *1405*, 8258.
45. de Almeida, A.K., Jr.; Prado, A.F.B.A. Comparisons between the circular restricted three-body and bi-circular four body problems for transfers between the two smaller primaries. *Sci. Rep.* **2022**, *12*, 4148. [CrossRef] [PubMed]
46. Fieseler, P.D. A method for Solar Sailing in a low Earth Orbit. *Acta Astronaut.* **1988**, *43*, 531–541. [CrossRef]